The RAPGAP Monte Carlo for Deep Inelastic Scattering

version 2.08/00

H. Jung
University of Lund, Department of Physics, Sweden

March 6, 2001

Abstract

The physics behind the Monte Carlo event generator RAPGAP are discussed, which includes deep inelastic scattering, non - diffraction, diffraction and π - exchange as well as resolved virtual processes.

A detailed program description is given, with emphasis on parameters the user wants to change and common block variables which completely specify the generated events. Subroutines for initial state parton showers, remnant treatment and structure functions developed for LEPTO and PYTHIA have been copied and modified for the use in RAPGAP.

1 Tabular Summary

program name	RAPGAP
version	2.08/00
date of latest version	June 1999
author	Hannes Jung (Hannes.Jung@desy.de)
program size	$\sim$ 12000 lines of code
input files needed	none
computer types	any with standard Fortran 77, tested on SGI, HP-UX, SUN, IBM-PC
operating systems	Unix, Linux
applicability	Deep Inelastic ep Scattering
	Deep Inelastic ep Scattering with resolved photons
	Deep Inelastic Diffractive ep Scattering
	Deep Inelastic ep Scattering with π exchange
	Photo-production in ep Scattering
	Diffractive photo-production in ep Scattering
	Photo-production in ep Scattering with π exchange
hard sub-processes included	$eq \to e'q'$
	$eq \to e'qg$
	$eg \to e'q\bar{q}$
	$eg \to e'c\bar{c}$
	$eg \to e'b\bar{b}$
	$\gamma q \to qg$
	$\gamma g \to q\bar{q}$
	$\gamma g \to c\bar{c}$
	$gg \to gg$
	$qg \to qg$
	$q\bar{q} \to gg$
	$q\bar{q} \to q\bar{q}$
	$qq \to qq$
QCD cascade	initial and final state parton shower or
	ARIADNE
initial QED radiation	via HERACLES
fragmentation model	LUND string
other programs called	HERACLES 4.4
	JETSET 7.4
	ARIADNE 4
	BASES 5.1
	PDFLIB 7.09 (CERN Library)
availability	`http://www-h1.desy.de/~jung/rapgap.html`

2 Introduction

In high energy physics Monte Carlo Event Generators are heavily used to compare experimental data with theoretical predictions. For example in QCD the interaction between quarks and gluons can be calculated in leading - or next-to-leading order in the strong coupling constant α_s. In experiments only stable particles are measured, but not partons (quarks or gluons), which cannot be described by perturbation theory, because the coupling constant α_s becomes large at scales of the order of the mass of hadrons. Thus the hadronization has to be described by phenomenological procedures, for example with the hadronization packages JETSET [1, 2, 3] or HERWIG [4].

A typical Monte Carlo Event Generator usually starts by generating the momenta of the partons involved in the interaction according to a theoretical prescription. Such a typical event record could look like the following (from the JETSET event record):

Event listing (summary)

I	particle/jet	KS	KF	orig	p_x	p_y	p_z	E	m
1	!e-!	21	11	0	0.000	0.000	156.843	156.843	0.001
2	!p+!	21	2212	0	0.000	0.000	-156.843	156.846	0.938
3	!gamma!	21	22	1	1.819	18.493	4.371	3.243	-18.812
4	e-	1	11	1	-1.819	-18.493	152.472	153.601	0.001
5	!u!	21	2	2	0.000	0.000	-23.242	23.242	0.000
6	u A	2	2	5	1.820	18.496	-18.874	26.488	0.006
7	ud_0 V	1	2101	2	0.000	-0.003	-133.599	133.600	0.579
		sum:	0.00		0.000	0.000	0.000	313.689	313.689

The process described by this event record is deep inelastic electron proton scattering in the electron proton center of mass frame. The first two lines show the beam particles. A status code KS indicates whether the particle (or parton) is kept only for documentation (`KS = 21`) or whether it is a final state particle (parton) (`KS = 1`). The flavor code KF identifies uniquely the particle/parton. The row `orig` shows the line number of mother particle/parton. The third line in this example gives the exchanged virtual photon and the fourth line the scattered electron. In line 5 the parton of the proton struck by the virtual photon is given. Line 6 describes the scattered quark and in line 7 the remnant of the proton is given.

The partons in line 6 and 7 hadronize into visible particles. Of course the incoming parton (line 5) could be a result of QCD radiation from another parton with larger energy. Also the scattered parton (line 6) could radiate further partons before the actual hadronization takes place. Such an example is shown in the following, where both the initial and scattered partons are the result of further QCD radiation.

```
                              Event listing (summary)

 I  particle/jet KS     KF orig    p_x      p_y      p_z       E        m

 1  !e-!         21     11    0    0.000    0.000 -156.843  156.843    0.001
 2  !p+!         21   2212    0    0.000    0.000  156.843  156.846    0.938
 3  !gamma!      21     22    1    1.819   18.493   -4.371    3.243  -18.812
 4  e-            1     11    1   -1.819  -18.493 -152.472  153.601    0.001
 5  !u!          21      2    2   -0.358    0.403   81.763   81.764    0.000
 6  !u!          21      2    5   -0.069    0.246   28.064   27.754   -4.167
 7  !u!          21      2    4    1.797   19.188   21.113   28.585    0.006
 8  u          A  2      2    0   -1.648    8.569    8.978   12.520    0.006
 9  g          I  2     21    0    1.795    7.372    8.854   11.660    0.000
10  g          I  2     21    0    0.220    1.524    2.027    2.545    0.000
11  g          I  2     21    0    1.383    1.273    3.833    4.269    0.000
12  g          I  2     21    0    0.506    0.921    1.696    1.995    0.000
13  g          I  2     21    0   -0.559   -0.917   51.687   51.699    0.000
14  ud_0       V  1   2101    2    0.122   -0.249   75.397   75.400    0.579
              sum:  0.00          0.000    0.000   -0.001  313.689  313.689
```

In this example the first 4 lines are the same as above, but line 5 now shows the momentum of the parton originating from the proton before any QCD radiation, and line 6 gives the parton struck by the virtual photon (after initial state QCD radiation). Another difference to the first example is that a small primordial transverse momentum has been added to the parton originating from the proton. In line 7 the scattered parton is shown before any final state QCD radiation, whereas in line 8 the final parton after radiation is given. The partons radiated both from initial state and final state are given in the lines following line 8.

More details on how to generate events according to theoretical distributions, the basic physics processes and the way higher order QCD processes are simulated via parton shower cascades are given in the following sections.

3 Basics for Monte Carlo Generators

In Monte Carlo Event Generators one usually wants to calculate the cross section for various processes with the possibility to impose experimental cuts and to generate events according to theoretical distributions. These two subjects are closely related to each other.

First let us consider the integration of a function $f(x)$ with a Monte Carlo method. Having two independent random numbers, say R_1 and R_2, generated uniformly in the interval $(0,1)$, then we can calculate x_R with $x_R = x_{min} + R_1 \cdot (x_{max} - x_{min})$ and f_R with $f_R = R_1 \cdot f_{max}$. The integral $\int_{x_{min}}^{x_{max}} f(x)dx$ can be approximated by the sum of $\sum f_R$ for which $f_R < f(x_R)$. However, if the function $f(x)$ is strongly peeked at some value of

x, then this method becomes rather inefficient, because most of the time we will have $f_R > f(x_R)$ and thus the pair of random numbers has to be rejected.

The efficiency will increase, if we can generate x values according to some approximation of $f(x)$ by another function $g(x)$ which is much simpler and analytically integrable. Now we generate x values according to the function $g(x)$. This is done by the following:

$$R_1 \int_{x_{min}}^{x_{max}} g(x)dx = \int_{x}^{x_{max}} g(x)dx$$

Thus if we can integrate $g(x)$ analytically then the equation can be solved for x and we have then x generated according to $g(x)$. Let us assume $f(x)$ can be approximated by a function $g(x) = 1/x$. Then we have:

$$R_1 \int_{x_{min}}^{x_{max}} g(x)dx = R_1 \log \frac{x_{max}}{x_{min}} = \log \frac{x_R}{x_{min}}$$

Solving this equation we obtain $x_R = x_{min}(\frac{x_{max}}{x_{min}})^{R_1}$. In order to calculate the integral we proceed as follows:

$$\int f(x)dx = \int \frac{f(x)}{g(x)} g(x)dx \simeq \sum_i \frac{f(x_{R_i})}{g(x_{R_i})} \int g(x)dx$$

Because of the choice $f(x) \sim g(x)$, the ratio $\frac{f(x)}{g(x)}$ is more or less constant and independent of x. In the example with $g(x) = 1/x$ the integral is given by:

$$\int f(x)dx \simeq \sum_i x_{R_i} f(x_{R_i}) \log \frac{x_{max}}{x_{min}} \tag{1}$$

which can be easily calculated.

Now to generate x values according to $f(x)$ we use the same trick as above: first generate x according to the simple function $g(x)$ and then reject those values of x for which $\frac{f(x)}{g(x)} > R_2$. With this procedure x values are generated according to the function $f(x)$. Moreover this scheme is easily extended to the case of more than one dimension: for each variable $x_1, x_2, \ldots, x_n$ the same procedure is applied.

In RAPGAP the BASES [5] integration package is used. This package performs a Monte Carlo integration and according to a given function $f(y_i)$, it generates the variables y_i after internally optimizing a grid. In RAPGAP the random numbers x_i are generated with BASES but they are transformed to the variables y_i according to the procedure described above. Actually the variables y_i are the kinematic quantities y, Q^2, x_g, $x_{I\!P}$, t, ... given in the next section. In all cases the true distribution is approximated by $g(y_i) = 1/y_i$ and the weighting factor (eq.(1)) is applied. This procedure has the advantage of being very efficient, because BASES is used only to optimize the normally small difference between the approximated and the true function.

4 Cross Section and Partonic Subprocesses

4.1 Standard Deep Inelastic Scattering

The inclusive cross section for $e\ p$ deep inelastic scattering is given in terms of the structure function $F_2^p(x,Q^2)$ and the longitudinal structure function $F_L^p(x,Q^2) = F_2^p(x,Q^2) - 2xF_1^p(x,Q^2)$:

$$\frac{d\sigma(ep \to e'X)}{dy\,dQ^2} = \frac{4\pi\alpha^2}{yQ^4}\left(\left(1-y+\frac{y^2}{2}\right)F_2^p(x,Q^2) - \frac{y^2}{2}F_L^p(x,Q^2)\right) \tag{2}$$

with x defined as $x = Q^2/(2P.q)$, $y = (P.q)/(P.l)$ and $Q^2 = -q^2 = -(l-l')^2$ where P is the initial proton four vector, $q = l - l'$ is the four vector of the virtual photon with l (l') the four vectors of the initial (scattered) electron.

In the QCD improved quark - parton model for deep inelastic scattering the structure function F_2^p is given in terms of the corresponding parton distribution functions:

$$F_2^p(x,Q^2) = \sum_f e_f^2\left(xq_f(x,Q^2) + x\bar{q}_f(x,Q^2)\right) \tag{3}$$

where the sum runs over all quark flavors and $q_f(x,Q^2)$ ($\bar{q}_f(x,Q^2)$) gives the probability of finding a quark (antiquark) of flavor f with a momentum fraction x of the initial proton momentum.

Different parameterization of the parton densities in the proton can be selected in RAPGAP (via `MSTP(51)`) and the PDFLIB [6, 7] can be accessed.

4.2 Deep Inelastic Diffractive Scattering and pion exchange

In diffractive scattering (or pion exchange scattering) the inclusive cross section is given by [8]:

$$\frac{d^4\sigma(ep \to e'Xp')}{dy\,dQ^2\,dx_{I\!P}\,dt} = \frac{4\pi\alpha^2}{yQ^4}\left(\left(1-y+\frac{y^2}{2}\right)F_2^{D(4)}(x,Q^2;x_{I\!P},t) - \frac{y^2}{2}F_L^{D(4)}(x,Q^2;x_{I\!P},t)\right) \tag{4}$$

where the diffractive structure functions $F_2^D(x,Q^2;x_{I\!P},t)$ and $F_L^D(x,Q^2;x_{I\!P},t)$ are introduced, depending now on four variables, x, Q^2 defined as above and $x_{I\!P} = (q.p_{I\!P})/(q.P)$ and $t = (P-P')$ with P' being the four momentum of the elastically scattered outgoing proton. In the case of pion exchange (instead of pomeron exchange) one simply has to replace $F_{2;\,L}^D$ by the corresponding $F_{2;\,L}^\pi$ and $x_{I\!P}$ by x_π.

The interpretation of the diffractive structure function F_2^D in terms of parton distribution functions, in analogy to the proton structure function, is not that clear and different approaches exist [9]:

- **Resolved pomeron a la Ingelman and Schlein**

  In the model of Ingelman and Schlein [10] diffractive scattering is described in terms of pomeron $I\!P$ exchange, where the pomeron has a partonic structure. The structure function F_2^D is then given as the product of the probability for finding a pomeron $f_{p\,I\!P}$ and the structure function $F_2^{I\!P}$ of the pomeron:

$$F_2^{D(4)}(\beta, Q^2; x_{I\!P}, t) = f_{p\,I\!P}(x_{I\!P}, t) F_2^{I\!P}(\beta, Q^2) \tag{5}$$

  with $\beta = Q^2/(2q.p_{I\!P})$. In analogy to the quark - parton - model of the proton β can be interpreted as the momentum fraction of the total pomeron momentum carried by the struck quark and $F_2^{I\!P}(\beta, Q^2)$ can be seen as the quark probabilities in the pomeron. Different parameterization of the parton densities of the pomeron can be selected (`NG` with details given in the program description). The probability for finding a pomeron in the proton is available in three different parameterization.

  The parameterization of Streng and Berger et al. [11, 12, 13] can be obtained with `NPOM=0`:

$$f_{p\,I\!P}(x_{I\!P}, t) = \frac{\beta^2_{p\,I\!P}(0)}{16\pi} x_{I\!P}^{1-2\alpha_{I\!P}(t)} e^{-b_0|t|} \tag{6}$$

  with $\beta^2(0) = 58.74$ GeV^2 and $\alpha_{I\!P} = \alpha_{I\!P}(0) + \alpha'_{I\!P} t$ and $\alpha_{I\!P}(0) = 1 + \epsilon$ describing the pomeron trajectory with ϵ =`EPSP`, $\alpha'_{I\!P}$ =`ALPHP` and b_0 =`RN2` being free parameters.

  The parameterization of Ingelman and Bruni [14, 15, 16] is given (`NPOM=1`):

$$f_{p\,I\!P}(x_{I\!P}, t) = \frac{1}{2}\frac{1}{2.3}\frac{1}{x_{I\!P}} \left[6.38 e^{-8|t|} + 0.424 e^{-3|t|}\right] \tag{7}$$

  Donnachie and Landshoff [17] give the following (via `NPOM=2`) :

$$f_{p\,I\!P}(x_{I\!P}, t) = \frac{9\delta^2}{4\pi^2} [F_1(t)]^2 \, x_{I\!P}^{1-2\alpha_{I\!P}(t)} \tag{8}$$

  with $\delta^2 = 3.26$ GeV^2 and the elastic form factor $F_1(t)$:

$$F(t) = \frac{4m_p^2 - 2.8t}{4m_p^2 - t} \frac{1}{(1 - t/0.7)^2} \tag{9}$$

- **Resolved pomeron a la Ingelman and Schlein with a parameterization to H1 data**

  In [18] the H1 collaboration has given a parameterization of the diffractive structure function in terms of pomeron and meson trajectories. This parameterization can be selected by `NG=-10,-11,-12` for the NLO parameterizations and by `NG=-13,-14,-15` for the LO ones, according to a different ansatz for the parton distribution in the pomeron at the starting scale for the Q^2 evolution: `NG=-10` assumes only quarks at the starting scale Q_0, `NG=-11` has quarks and gluons, whereas in `NG=-12` a gluon distribution peaked at large values ξ, the parton momentum fraction, is assumed.

With `NPOM=-10` the predefined flux for pomeron exchange is selected, `NPOM=-11` gives the meson contribution only, and `NPOM=-12` gives the mix of pomeron and meson as obtained by the H1 collaboration [18].

- **Two gluon exchange for diffraction**

  This approach is mainly intended to describe exclusive high p_t di-jet production, but in the model of [19] estimates on the total inclusive diffractive cross section are given. The calculation of diffractive di-jet production can be performed using pQCD for large photon virtualities Q^2 and high p_t of the $q(\bar{q})$ jets [19, 20, 21, 22, 23, 24].

  The process is mediated by two gluon exchange. Different assumptions on the nature of the exchanged gluons can be made: in [20, 21] (`NG=42`, `NPOM=42`) the gluons are non perturbative, in [19] (`NG=40`, `NPOM=40`) they are a hybrid of non perturbative and perturbative ones and in [23, 24] (`NG=41` and `NPOM=41` or `IPRO=21`, which is done technically different and is more efficient) they are taken from a NLO parameterization of the proton structure function [25, 26]. The cross section is essentially proportional to the proton gluon density squared: $\sigma \sim [x_{I\!P} G_p(x_{I\!P}, \mu^2)]^2$ with μ^2 the scale explicitly given in the references.

  Due to the different gluon densities different $x_{I\!P}$ dependencies of the cross sections are expected and further discussed in [22], where also numerical estimates are presented.

- **Semi-classical approach of Buchmüller, McDermott and Hebecker**

  In [27] Buchmüller et al. ddefine an effective diffractive gluon density:

$$x_{I\!P} G^D(x_{I\!P}, \beta) = \frac{C_1}{\beta \cdot C_g - \beta + 1} \cdot \frac{1}{x_{I\!P}} \tag{10}$$

  with C_1 and C_g being free parameters. In addition the dipole form factor for the t dependence is applied. Note that with $C_g = 1$ a constant gluon density is obtained. In that approach there is only a $1/x_{I\!P}$ dependence in contrast to the other models, where at least a $1/x_{I\!P}^{1+\epsilon}$ is present.

- **Nikolaev Zakharov model for diffraction**

  A parameterization of the diffractive structure function in the model of Nikolaev and Zakharov [28] can be selected (`NG=30`, `NPOM=30`). In the implementation in RAPGAP only QPM type events can be generated, no higher order QCD processes like QCD-C or BGF are possible for `NG=30`, `NPOM=30`.

- **User defined model for diffraction**

  The user can freely define his preferred model for diffraction by supplying an effective diffractive structure function (`SUBROUTINE USDIFFR`). Here no assumption about factorization is made.

  The basic partonic subprocesses available are: $eq \to e'q'$ (QPM), $eq \to e'qg$ (QCD-C), $eg \to e'q\bar{q}$ (BGF), $eg \to e'c\bar{c}$ (BGF), $eg \to e'b\bar{b}$ (BGF), which are discussed in more detail in the following sections.

In all cases there is the possibility to add primordial p_T (via switch `IALMKT=1`) according to $\exp(-5.5 \cdot p_T^2)$ to the partons when process $IPRO = 12$ is selected.

4.3 Deep Inelastic Scattering including Diffraction and Pion exchange

Inclusive deep inelastic scattering obviously includes diffraction and π exchange etc. The total cross section of DIS, F_2, can be written as a sum of diffractive and non - diffractive contributions:

$$F_2(x, Q^2) = F_2^{non-diff}(x, Q^2) + F_2^{diff}(x, Q^2) + \ldots \tag{11}$$

where the dots indicate that other exchanges like pion exchange etc. can be treated similarly.

The diffractive contribution to F_2 is given by F_2^{diff}:

$$F_2^{diff}(x, Q^2) = \int F_2^{D(4)}(x_{I\!P}, t; \beta, Q^2)\delta(\beta x_{I\!P} - x)\, dx_{I\!P}\, d\beta\, dt \tag{12}$$

With the knowledge of F_2 and F_2^{diff} the non - diffractive part can be calculated which is then used in the Monte Carlo to generate the proper mix of diffractive and non - diffractive processes (`IDISDIF=1`). Similarly non - diffraction, diffraction and pion - exchange are selected with `IDISDIF=2`.

4.4 QED radiative corrections

Real photon emission from both the incoming and scattered electron can have large effects on the reconstruction of the DIS kinematic variables x, Q^2, y. These QED radiative effects are simulated with the HERACLES event generator [29, 30]. HERACLES is used to generate the $e-\gamma^*-e$ vertex including photon emission from the incoming and outgoing electron as well as virtual corrections. The interface to HERACLES is switched on with `IPRO=1200(1400)` to generate QED radiative effects for processes `IPRO=12(14)`

Since QED radiative effects tend to lower the actual Q^2 of the photon which is available for any subsequent process, one has to ensure that parton densities behave well at very small Q^2. In the quark parton model the QPM process has to vanish for $Q^2 \to 0$. On the other hand parton densities are usually only parameterized down to a fixed value of Q_0^2. In order to ensure a well defined small Q^2 behavior, a exponential suppression factor is applied: $1 - \exp(-\texttt{Q2SUPP} \cdot Q^2)$ with `Q2SUPP=3.37` being the default from HERACLES. Values of `Q2SUPP=5` seems appropriate for parton densities evolved down to $Q_0^2 \sim 1$ GeV^2 and `Q2SUPP=10` for $Q_0^2 \sim 0.5$ GeV^2.

4.5 Order α_s matrix elements

With the knowledge of F_2 the total cross section can be described in terms of scattering a virtual photon on a quark or antiquark. However this quark may have been originated from another parton, usually described by the Q^2 dependence of the parton densities resulting in a different hadronic final state. The process where a initial parton carrying a momentum fraction x_i, splits into other partons which then hard scatter with the photon, can be simulated in QCD parton showers (selected via `IFPS`) , for incoming (`IFPS = 1`), outgoing partons (`IFPS=2`) and both (via `IFPS = 3`). These QCD parton showers are based on the leading log DGLAP [31, 32, 33, 34] splitting functions in leading order α_s.

A more detailed simulation of leading order α_s processes like $\gamma^* g \to q\bar{q}$ (BGF, Fig. 1c.) and $\gamma^* q \to qg$ (QCD - compton, Fig. 1d.) can be obtained when the exact matrix elements for these processes are included.

These processes can be simulated separately with `IPRO = 13` for BGF (light quarks), `IPRO=14` for BGF (heavy quarks) and `IPRO = 15` for QCD-C.

A full simulation including QPM - as well as 1st order α_s - processes is selected with `IPRO=12` (or `IPRO =1200` for HERACLES) together with `IFULL=1`. The decision whether to generate a QPM or a 1st order α_s event is based on the cross section for a particular process at a given x and Q^2. Therefore for each event the cross section for BGF light quarks, BGF heavy quarks and QCD - Compton has to be obtained by numerical integration including the proper parton densities. If the scale chosen for α_s and the parton densities (`IQ2`) is Q^2 or $\hat{s}$, then the matrix elements are integrated analytically over z leaving only a one dimensional numerical integration. If, however, the scale is p_T^2 (or any function of it) then α_s and the parton densities cannot be factorized, and a time consuming two dimensional numerical integration has to be performed. As an alternative the QCD probabilities are calculated once and stored in a grid (`IGRID=1`). This approach is faster but less accurate. This procedure is recommended if the scale is chosen to be p_T^2 (`IQ2=3`) or $Q^2 + p_T^2$ (`IQ2=5`).

In order to avoid divergences in the matrix elements for massless quarks a cutoff in p_T^2 has to be specified (`PT2CUT`). The minimum p_T^2 is only restricted by the requirement that the sum of the order α_s processes is smaller or equal F_2.

However care has to be taken in the case of pomeron exchange, that Q^2 evolved parton densities are used with the proper normalizations for quark and gluon densities, otherwise it can occur that the probability for photon - gluon fusion exceeds the total cross section calculated from F_2^{IP} with the quark densities even for relatively large `PT2CUT`.

4.6 Treatment of heavy flavor production

Heavy flavors, like charm and bottom, are usually produced via boson - gluon fusion. However in the evolution of the parton densities, and similarly in the evolution of $F_2(x, Q^2)$, heavy quarks are often treated in the same way as light quarks, often not even respecting the production threshold properly. Thus when calculating 1st order α_s

matrix elements there is a contribution of QCD-C from charm in the proton, together with BGF and eventually also QPM type events with charm. Whether this is a consistent treatment, depends on the details of the Q^2 evolution of the parton densities.

GRV [25, 26], for example, calculate $F_2^{charm}(x,Q^2)$ only via BGF. Thus in their approach the charm quark density is zero. However, for technical reasons for calculation of the total cross section, in the parameterization of the parton densities, as implemented in PDFLIB [35] a charm quark density is provided, which is calculated from the BGF process. This is correct as long as only the total cross section is considered, which is calculated via

$$\sigma^{\gamma^* p}(x,Q^2) = \frac{4\pi^2\alpha}{Q^2} \cdot F_2(x,Q^2) = \frac{4\pi^2\alpha}{Q^2} \cdot \sum_{i=-6}^{6} e_i^2 \cdot xq_i(x,Q^2) \tag{13}$$

For a proper description of the hadronic final state using the GRV parton densities, only light quarks are allowed for QPM and QCD-C processes, and all heavy quarks are only produced via BGF.

Just from the parton density parameterization itself, it is nor possible to decide whether heavy quarks are produced only via BGF or not. Thus the user has to take care of this via `NFLQCDC`, which is set by default to `NFLQCDC=3`. If heavy quarks are allowed to be produced also by QCD-C processes, then the user should set `NFLQCDC=4`, or `NFLQCDC=5`.

4.7 Resolved Photons in DIS

Resolved photon processes play a important role in high p_T jet - production in photo-production. Any internal structure in the proton as well as in the photon can be resolved as long as the scale of the hard subprocess, which is of the order of p_T^2, is larger than the inverse radius of the proton $1/R_p^2 \sim \Lambda_{QCD}^2$ and the photon $1/R_\gamma^2 \sim Q^2$.

In DIS resolved photon processes [36] can play a role when the scale μ^2 of the hard subprocess is larger than Q^2, the inverse size of the photon.

Resolved photon processes in DIS are more complicated than in photo-production because one has to treat properly the kinematics of the scattered electron. This is done with the Equivalent Photon Approximation, giving the flux of virtual transverse polarized photons [37, and references therein]. The structure of the virtual photon is defined by parameterizations of the parton densities of the virtual photon, now depending on the scale μ^2 and Q^2: $x_\gamma f_\gamma(x_\gamma, \mu^2, Q^2)$ [38, 39, 40]. Resolved photon processes can be selected via `IPRO=18` for real and virtual photons (depending on Q^2_{min}). The hard subprocesses implemented in RAPGAP are:

$$gg \to q\bar{q} \qquad \texttt{IRPA=1} \tag{14}$$

$$gg \to gg \qquad \texttt{IRPB=1} \tag{15}$$

$$qg \to qg \qquad \texttt{IRPC=1} \tag{16}$$

$$q\bar{q} \to gg \qquad \texttt{IRPD=1} \tag{17}$$

$$q\bar{q} \to q\bar{q} \qquad \texttt{IRPE=1} \tag{18}$$

$$qq \to qq \quad \texttt{IRPF=1}. qq \to qq(BFKL) \quad \texttt{IRPG=1}. \tag{19}$$

The corresponding color configurations are given in `ICOLORA`.

Since this processes can only occur for $\mu^2 > Q^2$, large differences in the cross section are expected when choosing different scales μ^2, like $\mu^2 = p_t^2$, or $\mu^2 = \hat{s}$. A part of this dependence is removed when next-to-leading order diagrams are considered. For example the process $qg \to qg$ also occurs in a NLO calculation for jet production in DIS [41, 42, 43]. However in resolved photon processes there is also the evolution of the virtual photon parton densities from Q^2 to the scale μ^2, which is a resummation to all orders. Therefore differences between full NLO calculations and resolved photon processes are expected [43].

From version 2.06/29 resolved photon processes are also implemented for diffraction and π exchange.

4.8 Scales, α_s and Parton Distribution Functions

In leading order α_s processes the renormalization scale μ_R ($\alpha_s(\mu_R^2)$) and factorization scale μ_F ($xf(x,\mu_F^2)$) are not well defined, and any choice of $\mu_R^2 = \mu_F^2 = Q^2,\ p_t^2,\ 4p_t^2,\ \hat{s},\ Q^2+p_t^2$ is reasonable. There are essentially two competitive effects: a larger scale gives smaller $\alpha_s(\mu^2)$ but a larger parton density $xf(x,\mu^2)$ at fixed x. The net effect depends on the details of the interaction and the parton density.

RAPGAP offers different choices for the scales: $\mu^2 = m^2,\ \hat{s},\ m^2+p_t^2,\ Q^2,\ Q^2+p_t^2$, selected with `IQ2 = 1,...,5` (`IQ2=1` only makes sense for heavy quark production). A scale factor `SCALF` can be chosen to study the effect of different scales: `SCALF=4` with `IQ2=3` will result in a scale $\mu^2 = 4p_t^2$ for α_s and the parton densities. In case of `IQ2=5` a scale factor `SCALF=4` will result in $\mu^2 = Q^2 + 4 \cdot p_t^2$.

Considering the $O(\alpha_s)$ matrix element processes one could argue that the scale corresponds to the propagator t (u for the crossed diagram) [44], which is

$$\begin{aligned} \mu^2 &= \max(|t,u|) && (20)\\ &= \max(|-Q^2-2q.p_{f\,1}, -Q^2-2q.p_{f\,2}|) && (21)\\ &= \max(1-z,z)\cdot\left(\hat{s}+Q^2\right) && (22) \end{aligned}$$

with $z = \frac{p_i.p_{f\,1}}{p_i.q}$ and p_i (p_f) being the momentum of the initial (final) state parton. Expressing p_T^2 in terms of z it is easily seen that this choice of the scale μ^2 is always larger than $p_T^2 = z(1-z)\hat{s}$.

The strong coupling constant is calculated consistently in the one loop expression (using `ULALPS` from JETSET [1, 2, 3]):

$$\alpha_s(\mu^2) = \frac{12\pi}{(33-2n_f)\log(\mu^2/(\Lambda_{QCD}^{n_f})^2)}$$

Often Λ_{QCD} is just taken from the parameterization of the parton densities, but when using non - diffractive processes together with diffraction and pion exchange, it is not

clear which Λ_{QCD} to take, the one from the parameterization of the proton, the pomeron or the pion. The same problem occurs when resolved photon processes are included. In RAPGAP, the value for Λ_{QCD} has to specified separately via the switches of JETSET: `MSTU(112)` giving the No. of flavors with respect to Λ_{QCD}, `PARU(112)` giving the value of Λ_{QCD}. The default value is $\Lambda^5_{QCD} = 0.25$ and `MSTU(112)=5`. The number of actual open flavors n_f depends on μ^2, and α_s is required to be continuous at the flavor thresholds.

Most recent parton density parameterizations of the proton and the pion can be accessed from the PDFLIB [6, 7] with `MSTP(51)=1000000*NPTYPE` 1000*NGROUP + NSET+ (example: `MSTP(51)=1005007` gives GRV HO structure function of the proton). Technically `PYSTFU` from PYTHIA [3] has been modified to be used within RAPGAP. If the user has no access to PDFLIB internally coded parameterizations can be used with `MSTP(51)<10` with details given in the program description.

The parton densities of the pion are accessed similarly with `MSTP(52)`.

The parton densities of the virtual photon are accessed with `MSTP(56)`. In the program the parameterizations GRS [38] (`MSTP(56)=1`) and SaS [39] (`MSTP(56)=2`) are available. For `MSTP(56)>10` again PDFLIB is used for real photons and the virtual photon suppression factor of Drees - Godbole [40] is applied.

In the resolved photon case a factor `SCALQ2` can be specified, which regulates the phase space region, where resolved photon processes are possible: `SCALQ2=1` means $\mu^2 \geq 1 \cdot Q^2$, and `SCALQ2=10` means $\mu^2 \geq 10 \cdot Q^2$ where μ^2 is the scale specified by `IQ2`.

4.9 Exclusive Vector-meson Production

Vector meson production is included naturally in diffractive scattering. This is easiest seen for J/ψ production. Suppose we have a system of a $c\bar{c}$ quark, plus eventually additional gluons in the final state. If the invariant mass $m_x = (q + p_{I\!P})^2 < 4 \cdot m^2_{D^0}$ then only J/ψ's can be produced (η_c production is not possible because of spin constraints). Technically this is done in the fragmentation program JETSET [1, 2, 3]. However the ratio of spin 0 to spin 1 mesons has to be included by hand by setting `PARJ(13)=1` (for the light u, d mesons `PARJ(11)=1`, and for s mesons `PARJ(12)=1`) for JETSET. The production of the light vector-mesons ρ, ω and ϕ proceeds in a similar way to that of the J/ψ, but the ratio $\rho : \omega = 9 : 1$ has been included by hand by G. Briskin [45] in a modified subroutine `LUKFDI` of JETSET.

Exclusive vector meson production implies certain restrictions on the kinematic variables $x_{I\!P}$ and β:

$$x_{I\!P} = \frac{q.p_{I\!P}}{q.P} = \frac{Q^2 + m_x^2}{Q^2 + W^2}$$

$$\beta = \frac{Q^2}{2 \cdot q.p_{I\!P}} = \frac{Q^2}{Q^2 + m_x^2}$$

Thus for $m_x = m_{VM}$ and fixed W the variables $x_{I\!P}$ and β depend only Q^2. Thus changing Q^2 means moving in the two dimensional $x_{I\!P} - \beta$ plane, which has consequences on the Q^2 dependence of the $\gamma^* p \to \mathrm{VM}p$ cross section.

The cross section for vector meson production of course depends crucially on the underlying subprocess. Using the recent parameterization of $F_2^{D(3)}(x_{I\!P}, \beta, Q^2)$ of the H1 collaboration [18] together with `IPRO=12` and `IDIR=0` (which is QPM on a parton in the pomeron) J/ψ production as measured by the experiments H1 and ZEUS [46, 47] can be well described as a function of Q^2 and also W [48]. Surprisingly a $\sim 1/Q^4$ dependence of the photon proton cross section appears, which can be interpreted as a higher twist effect. However in the model described here this Q^2 dependence appears naturally from the β dependence of the structure function $F_2^{D(3)}$, since as shown above, changing Q^2 is equivalent with changing β for a given vector-meson.

5 Remnant Treatment and Fragmentation

The fragmentation in RAPGAP is done with the Lund - string model as implemented in JETSET [1, 2, 3]. For the treatment of the remnant and initial state parton showers, subroutines from the programs LEPTO 6.1 [44] (`LMEPS`, `LPRIKT`, `LREMH`) and PYTHIA [3] (`PYREMN`, `PYSPLI`, `PYSSPA`) have been copied and modified to be applicable here. The original structure of these subroutines is kept.

Optionally higher order QCD radiation can be simulated via leading log parton showers (`IFPS=1` for initial state parton shower, `IFPS=2` for final state PS, `IFPS=3` for initial and final state PS) or with the color dipole model (as implemented in ARIADNE [49] with `IFPS=10`).

5.1 Hadronic final state

In a standard inelastic scattering process a parton carrying color is removed from the target (a proton and/or a photon in case of resolved photon processes) and in general colored remnants are left. These remnants together with the colored partons of the hard interaction must form color singlet states (see Fig. 1). Color strings connect the colored partons with the remnants and these color strings generate particle flows between the remnants and the partons of the hard scattering.

In the lowest order process ($\gamma^* q \to q'$) the remnant is a $di-quark$ when the scattering occurs on a valence quark of the proton (Fig. 1*a*.). If, however, the scattering occurs on a sea quark or a anti - quark, the remnant is treated as a valence quark and valence $di-quark$ plus the corresponding anti - quark from the sea. This "new" sea quark treatment was first developed and implemented in LEPTO 6.5 [50] (Fig. 1*b*.).

In the case of BGF a color octet gluon is removed from the proton leaving a quark and a $di-quark$ behind. The quark from BGF forms a color string with the $di-quark$ and the anti - quark from BGF is connected via another string to the remnant valence quark (Fig. 1*c*.).

For QCD - Compton ($\gamma^* q_i \to q_f g_f$) the gluon g_f acts as a kick in the color string drawn from the quark q_f to the remnant $di-quark$ (Fig. 1*d*.). If the quark q_i actually

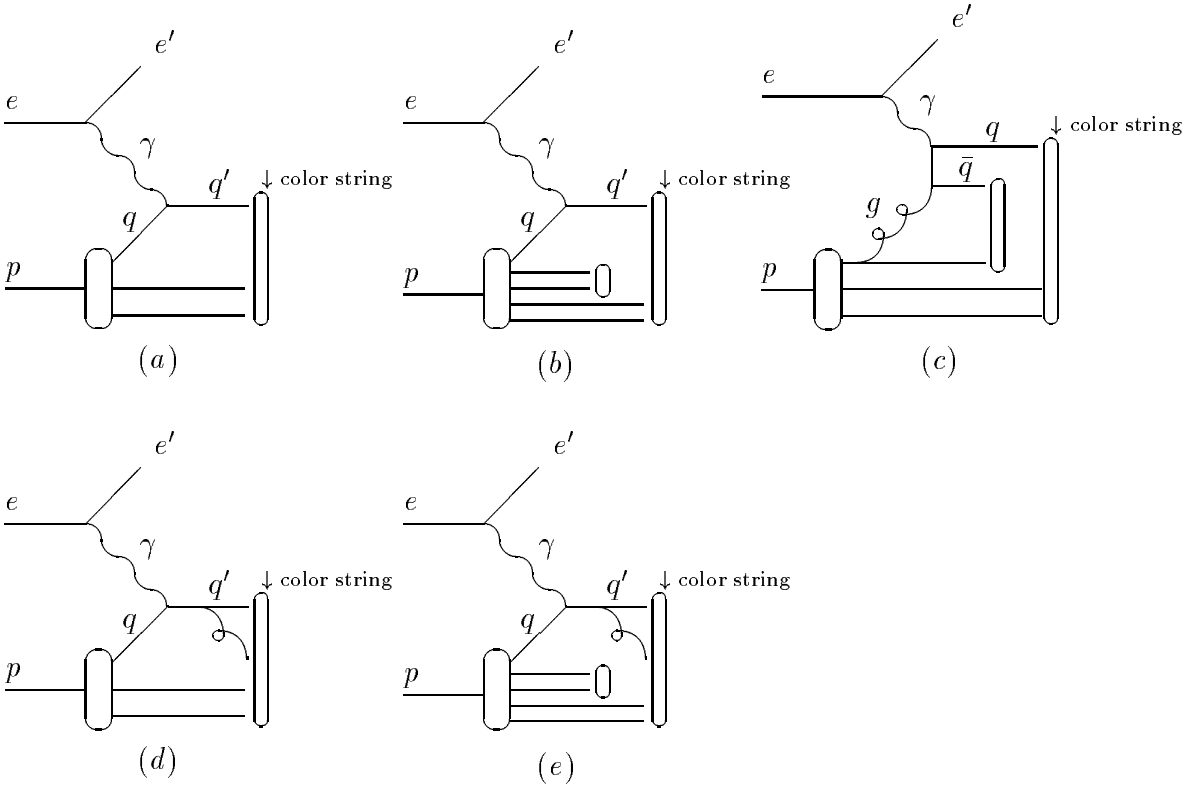

Figure 1: Basic processes for inelastic lepton nucleon scattering. Indicated are the color strings and the proton remnant. *a.* shows the lowest order process for scattering on a valence quark. The remnant of the proton is just a di - quark-quark. *b.* shows the lowest order process for scattering on a sea quark. The remnant of the proton is the corresponding anti-quark , a valence quark and a valence di-quark. *c.* shows the $O(\alpha_{em}\alpha_s)$ for gamma gluon fusion (the crossed diagram is not shown). The proton remnant is the valence quark and valence di-quark. *d.* shows the $O(\alpha_{em}\alpha_s)$ for QCD Compton (the crossed diagram is not shown) on a valence quark. The proton remnant is the same as in *a.* *e.* shows the $O(\alpha_{em}\alpha_s)$ for QCD Compton (the crossed diagram is not shown) on a sea quark. The proton remnant is the same as in *b.*

was a sea quark, then the remnant has an additional anti-quark $\bar{q}_i$. This anti-quark $\bar{q}_i$ forms a color singlet state with the left over valence quark q_v of the proton (Fig. 1*e.*). If the scattering occurred on a anti quark, then the strings are just reversed.

In rapidity gap events the proton stays intact or becomes a low mass diffractive state, here simply labeled with p'. Because of the emission of the color neutral particle there is no color connection between the outgoing scattered proton p' and the other particles.

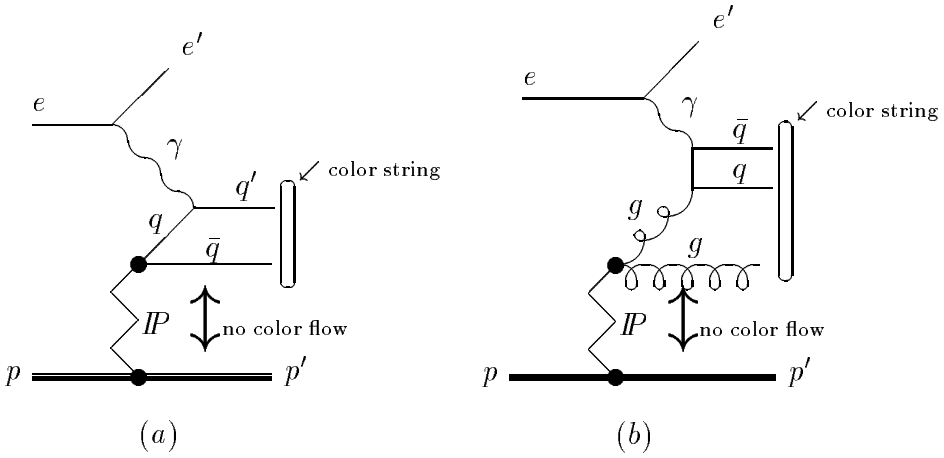

Figure 2: Basic processes for inelastic diffractive lepton nucleon scattering. Indicated are the color strings and the pomeron remnant. *a.* shows the lowest order process for scattering quark. *b.* shows the $O(\alpha_{em}\alpha_s)$ for gamma gluon fusion (the crossed diagram is not shown). The pomeron remnant is a color octet gluon *c.* shows the $O(\alpha_{em}\alpha_s)$ for QCD Compton (the crossed diagram is not shown) on a quark. The pomeron remnant is the same as in *a*.

When a quark (anti-quark) is removed from the pomeron a anti-quark (quark) of the same flavor but with the corresponding anti-color is left (Fig. 2a). When a gluon is removed from the pomeron $I\!P$, a color octet remnant is left, here treated as a single gluon. This pomeron remnant together with the $q\bar{q}$ of the hard interaction forms the color singlet state (Fig. 2b).

Pion exchange is treated similarly to pomeron exchange with the corresponding modifications for the outgoing particle p' which is a p, n or Δ^{++} corresponding to π^0, π^+ or π^- exchange. The treatment of valence and sea quarks follows the same principles as for inclusive ep scattering described above.

The color strings are much more complicated for resolved photon processes because two remnants, one from the proton and one from the photon, have to be considered. Resolved photon processes are similar to $p\bar{p}$ scattering and the relevant color connections are discussed in detail in [51].

5.2 Proton dissociation

Dissociation of the proton can be included for diffractive events via NFRAG=10. In this case the proton is split into a quark q_p and di-quark $di - q_p$ system, whereas the pomeron is assumed to couple to a single quark q_p only, and therefore the outgoing quark q_p' carries all of the momentum transfer t giving it a transverse momentum. The quark to which

the pomeron couples carries a momentum fraction χ of the protons initial momentum. The momenta of the initial quark q_p and the di-quark $di - q_p$ are given in the following:

$$\begin{aligned} q_p &\simeq \chi p & (23)\\ di - q_p &\simeq (1-\chi)p & (24)\\ q'_p &= q_p - p_{I\!P} \simeq \chi p - p_{I\!P} & (25) \end{aligned}$$

where $\chi = \frac{q.q_p}{q.p}$ with q (q_p, p) being the photon (quark, proton) momentum. In addition the quark and di-quark get primordial $p_\perp$ according to a Gaussian distribution.

The momentum fraction χ can be estimated within the resolved pomeron model:

$$\chi = \frac{x_{I\!P}}{\beta'} \tag{26}$$

with $\beta' = \frac{q.p_{I\!P}}{q.q_p}$ being the momentum fraction of the quark q_p of the pomeron momentum, and $x_{I\!P} = \frac{q.p_{I\!P}}{q.p}$. The value of $x_{I\!P}$ is already known from the interaction $\gamma I\!P$ and β' can be generated according to quark density of the pomeron.

For β' different probability functions are available:

$$\begin{aligned} P(\beta') = &\quad 2(1-\beta') && \texttt{(IREM=1)}, & (27)\\ P(\beta') = &\quad (a+1)(1-\beta')^a && \texttt{(IREM=2)}, & (28)\\ P(\beta') = &\quad \frac{N}{\beta'\left(1-\frac{1}{\beta'}-\frac{c}{(1-\beta')}\right)^2} && \texttt{(IREM=3)} & (29) \end{aligned}$$

with a chosen such that $< \beta' >= 1/(a+2)$ and c determined by the ratio of masses of the remnant quark and di-quark system. The option `IREM=1` corresponds to a hard quark density of the pomeron. Actually all the parameterizations are taken from inclusive DIS scattering as implemented LEPTO 6.1 [44].

The mass distribution M_R of the p - dissociative system follows in general a $1/M_R$ distribution for all the parameterizations of $P(\beta')$ available [48].

Even with proton dissociation switched on, a proton will emerge after fragmentation when the momentum transfer is small and the mass of the q - $di - q$ system remains below the threshold for multi-particle production.

5.3 QCD parton shower evolution

Higher order QCD effects are taken into account using the leading log parton shower approach.

5.3.1 Initial state radiation

Starting from the hard scattering process with x being the fractional momentum of the incoming quark at a suitable scale μ^2, a backward evolution according to the DGLAP evolution equations [31, 32, 33, 34] will lead to larger initial values of x_i and smaller μ^2. Especially at high center of mass energies initial state QCD radiation will become important and has to be taken into account to model properly the hadronic final state.

The probabilities for a branching of a parton $a \to bc$ to happen are given by the DGLAP evolution equations:

$$\frac{d\, f_a(x,t)}{d\, t} = \frac{\alpha_s(t)}{2\pi} \sum_a \int_x^1 \frac{d\, x'}{x'} f_a(x',t) P_{a\to bc}\left(\frac{x}{x'}\right) \tag{30}$$

where $f_a(x',t)$ are the parton density functions, giving the probability of finding a parton a carrying the fraction x' of the momentum fraction x probed at a scale t. $P_{a\to bc}$ are the DGLAP splitting functions:

$$P_{q\to qg}(z) = \frac{4}{3}\frac{1+z^2}{1-z} \tag{31}$$

$$P_{g\to gg}(z) = 6\frac{(1-z(1-z))^2}{z(1-z)} \tag{32}$$

$$P_{g\to q\bar{q}}(z) = \frac{1}{2}(z^2+(1-z)^2) \tag{33}$$

Soft gluon emission causes problems, since the splitting functions $P_{q\to qg}, P_{g\to gg}$ are divergent as $z \to 1$. Practically in order to avoid divergences, a upper cutoff z_{max} is introduced and the remaining soft gluon emission is treated as an effective shift in z (for details see [52, 53]). The actual value of $z_{max} = \frac{x+\epsilon}{x}$ plays a crucial role in properties of the hadronic final state, such as the transverse energy flow in the proton direction. Using the standard value of PYTHIA for ϵ, which is $\sqrt{s}\cdot\epsilon = 2$ GeV, the transverse energy in the proton direction in DIS away from the current jet falls well below the data [54]. Decreasing ϵ increases the transverse energy flow, and the data are much better described. The value z_{max} chosen in RAPGAP corresponds to the kinematic limit of quark pair creation when the current masses of the quarks are taken into account.

Starting from the hard interaction process at a suitable scale μ^2 ($\mu^2 = \hat{s}, p_\perp^2$) the partons are evolved backward. This backward evolution is quite complicated and is used in the Monte Carlo program for efficiency reasons when optimizing the generation of the kinematic variables for the hard scattering process. In a forward evolution scheme the number of degrees of freedom for the generation would vary event by event and no standard optimization procedure would be applicable.

In $p\bar{p}$ collisions the "$\hat{s}$ approach" is widely used (PYTHIA [52, 53]) whereas a different approach in lepto-production is adapted in LEPTO [55, 44]. The initiators of the parton shower cascade (partons inside the proton for example) are treated collinear with the original particle when effects from primordial k_t are neglected and have negligible mass ($m^2 \leq 1$ GeV). When a branching occurs, $p_3 \to p_1 + p_2$, the daughter partons p_1 and p_2

will have transverse momenta and virtualities greater than that of the initiator p_3. Thus after the QCD cascade the partons going into the hard interaction also have transverse momenta compared to the non parton shower case.

In γp and $p\bar{p}$ collisions there is no problem associated with this treatment since the kinematics of the hard interaction usually cannot be determined by measuring the scattered beam-particles either because the beam-particle is totally absorbed (the photon in γp) or because the beam-particle is insufficiently measured by experiment. However in lepto-production the kinematics are usually defined by the scattered lepton (y, Q^2 for example). In that case there will be mismatch between the generated y, Q^2 (before the parton cascade) and after QCD radiation has been added mainly because of the additional transverse momentum. For lepto-production a special approach has been developed "LEPTO approach" [55, 44]) in order to keep the scattered lepton and the (virtual) photon unchanged even with initial state parton shower. This approach is now consistently used in RAPGAP within the subroutine `PYSSPA` which was taken from PYTHIA and LEPTO [3, 44] with considerable modifications to be used also for low Q^2 processes, photo-production and diffractive scattering.

In DGLAP based parton showers the emitted partons are strongly ordered in p_T, meaning that in a backward evolution the parton with the largest p_T is generated first and closest in rapidity to the hard subprocess partons. The other partons generated must have smaller p_T.

If the hard scattering was just the lowest order process ($\gamma q \to q$) then the (only available and) largest scale is Q^2 and the p_T of the shower partons can go up to $\sqrt{Q^2}$. The situation is different when $O(\alpha_s)$ matrix element processes are considered. The maximum scale could be Q^2, $\hat{s}$, p_T^2. Here we choose the maximum scale to be:

$$\mu^2 = \max(|-Q^2 - 2q.p_{f\,1}, -Q^2 - 2q.p_{f\,2}|) \tag{34}$$

This choice [44] is motivated from the propagator of the matrix elements and is of the order of p_T^2 as shown in eq.(22).

When $O(\alpha_s)$ processes are considered in addition to the leading order process ($\gamma q \to q$) then the maximum scale for parton showers are calculated as follows: parton showers in the leading order process can go up to $\mu^2 = 4 \cdot p_{T\,cut}^2$ instead of Q^2 when no matrix elements are included (with $p_{T\,cut}^2 =$ `PT2CUT` being the divergency cut off in the matrix elements). This choice can be understood since parton emissions with $p_T > p_{T\,cut}$ are already included in the matrix element simulation [44]. Parton showers in the matrix element processes can go up to virtualities defined in eq.(22).

It is obvious that the initial state parton shower approach can only be applied correctly when parton densities are available as a function of Q^2. Moreover this parton densities have to be obtained in a consistent way using the DGLAP evolution equations and consistent definition of α_s.

Now also even for diffractive scattering QCD analysis of $F_2^{D(3)}$ and parameterizations of the diffractive parton densities obtained with DGLAP are available and can be used in initial state parton showers.

Optionally QCD cascades can be simulated according to the color dipole model as implemented in ARIADNE [49]) (via `IFPS=10`).

5.3.2 Final state parton showers

Final state parton showers are more easily simulated (LUSHOW of JETSET) since here a forward evolution scheme is used and no parton densities enter the evolution. The maximum scale is either $\min(4p_{T\ cut}^2, W^2)$ for the leading order processes or $\hat{s}$ for the $O(\alpha_s)$ matrix elements. Details can be found in [3].

6 Description of the program components

6.1 Subroutines and functions

RGMAIN	main program
GRAINI	initializes the program
RAPGAP	performs integration of the cross section. This routine has to be called before event generation can start.
RAEND	prints cross section and the number of events.
EVENT	performs the event generation and the proper mixing of parton shower and matrix elements if selected via IFULL=1. Also the mixing of *standard IS*, diffractive scattering and pion exchange is done, if selected via IDISDIF=1.
ANALYS	user analysis subroutine.
ALPHAS(RQ)	give $\alpha_s(\mu)$ with μ =RQ.
PARTI	initial particle and parton momenta are given.
DFUN	interface to FXN1
FXN1	calls routines for selected processes: DIFFR1, DIFFR2, DIFFR3, DIFFR4, DIS1, DIS2, DIS3, DIS4.
CUTG(IPRO)	cuts for process IPRO=13 and IPRO=15 (γg fusion and QCD - Compton) in integration and event generation.
FRAG	generates color string connection for hadronization.
DIFFR1	for diffractive and pion exchange processes $\gamma g_{I\!P} \to q\bar{q}$. Calls kinematics and phase space routine PARTDF and matrix element ELEQQL and ELEQQB. Both for light and heavy quarks. Using Equivalent Photon approximation and $\gamma g \to q\bar{q}$ matrix element.
DIFFR2	for diffractive and pion exchange processes $eg_{I\!P} \to e'q\bar{q}$. Calls kinematics and phase space routine PARTDF and matrix element ELEQQF. Both for light and heavy quarks. Using full matrix element for $eg \to e'q\bar{q}$.
DIFFR3	for diffractive and pion exchange processes $eq(\bar{q}) \to e'q'(\bar{q}')$. Calls kinematics and phase space routine PARTDF.
DIFFR4	for diffractive and pion exchange processes $eq_{I\!P} \to e'qg$. Calls kinematics and phase space routine PARTDF and matrix element ELEQCDC. Using full matrix element for $eq \to e'qg$.
DIS1	for *standard* inelastic scattering $\gamma g_p \to q\bar{q}$. Calls kinematics and phase space routine PARTDI and matrix element ELEQQL and ELEQQB. Both for light and heavy quarks. Using Equivalent Photon approximation and $\gamma g \to q\bar{q}$ matrix element.

DIS2 for *standard* inelastic scattering $eg_p \to e'q\bar{q}$. Calls kinematics and phase space routine PARTDI and matrix element ELEQQF. Both for light and heavy quarks. Using full matrix element for $eg \to e'q\bar{q}$.

DIS3 for *standard* inelastic scattering $eq(\bar{q}) \to e'q'(\bar{q}')$ Calls kinematics and phase space routine PARTDI.

DIS4 for *standard* inelastic scattering $eq_{I\!P} \to e'qg$. Calls kinematics and phase space routine PARTDI and matrix element ELEQCDC. Using full matrix element for $eq \to e'qg$.

ELEQQL matrix element for $\gamma g \to q\bar{q}$. q stands for light quark.

ELEQQB matrix element for $\gamma g \to Q\bar{Q}$ including masses. Q stands for heavy quark.

ELEQQF matrix element for $eg \to e'Q\bar{Q}$ including masses. Q stands for light or heavy quark. Masses of light quarks $m_q = 10$ MeV.

ELEQCDC matrix element for $eq \to e'qg$. Masses of light quarks $m_q = 10$ MeV.

ELERES matrix elements for resloved photon processes.

ELEQQ matrix element for exlusive diffractive $q\bar{q}$ production [23, 24].

ELEQQG matrix elements for diffractive $q\bar{q}g$ production [56].

DOT(A,B) A.B four vector dot product

DOT1(I,J) four vector dot product of vectors I and J in LUJETS common.

RANUMS vector of random numbers used in event generation.

PHASE phase space and generation for momenta of final partons in hard subprocess. $2 \to 2$ and $2 \to 3$ processes.

PARTDF phase space and event record for diffractive and pion exchange processes.

PARTDI phase space and event record for *standard* inelastic scattering processes.

PYSTFU(KF,X,SCALE,XPQ) parton density in particle KF (KF = 2212 for the proton). XPQ= $xf_i(x,\mu^2)$ with X= x, SCALE= μ^2. Copied from LEPTO 6.1 [44] and updated to include partons of the pomeron (pion) inside the proton.

RASTFU(KF,X,SCALE,XPQ) parton density in particle KF (KF = 100 for the pomeron, KF = 211 for the pion). XPQ= $xf_i(x,\mu^2)$ with X= x, SCALE= μ^2.

RAT2DI(KF,X,XMAX,TMIN,T,WTDIST) T= t and X= r dependent probability distribution for radiating a parton KF from the proton. (KF = 100 for the pomeron, KF = 211 for the pion).

PYREMN(IPU1,IPU2) routine for remnant treatment. Copied from LEPTO 6.1 [44] and updated for the use in resolved photon, diffractive and pion exchange processes.

PRODIFF routine for proton dissociation. The proton is treated as a quark diquark system.

PYSPLI(KF,KPA,KFSP,KFCH) give the spectator KFSP and KFCH partons when a parton KPA is removed from particle KF. Copied from LEPTO 6.1 [44] and updated for the use in resolved photon processes, diffraction and pion exchange.

`LMEPS` routine for color flow in all processes and preparation for initial and final state parton showers. Copied from LEPTO 6.1 [44] and updated for the use in low Q^2 processes, photo-production, resolved photon processes, diffraction and pion exchange.

`PYSSPA(IPU1,IPU2)` routine for initial state radiation. Calls LSCALE. Copied from LEPTO 6.1 [44] and updated for the use in low Q^2 processes, photo-production, resolved photon processes, diffraction and pion exchange.

`LSCALE` gives the maximum virtuality to be used for initial state parton shower generation. Copied from LEPTO 6.1 [44] and updated for the use for diffractive and pion exchange processes.

`GADAP` Gaussian integration routine for 1-dim and 2-dim integration. Copied from LEPTO 6.1 [44].

`RALMKT` generate primordial p_T according to the Aligned Jet Model.

`RYSTGA` master routine for parton densities of the virtual photon. Calls `GRSPAR` and `SASGAM`.

`GRSPAR` parameterization of Gluck, Reya, Stratman [38].

`SASGAM` parameterization of Schuler, Sjöstrand [39].

`F2DHW` calculation of diffraction for `NG=40` [19].

`F2BLW` calculation of diffraction for `NG=41` [23, 24].

`F2MD` calculation of diffraction for `NG=42` [20, 21].

`F2MCD` calculation of diffraction for `NG=45` [27].

`USDIFFR(BETA,SCALE,XPQ,X_POM,T2)` user supplied effective diffractive parton density with the fractional momentum `BETA`= ξ_i of the pomeron momentum carried by the parton i, the scale `SCALE`=μ of the structure function `XPQ(-6:6)`=$\xi q(\xi,\mu^2)$, `X_POM`= $x_{I\!P}$ and `T2`= t (all variables in `SINGLE PRECISION`).

6.2 Parameter switches

`IINT:` (D:=0) select integration procedure
=0 BASES/SPRING Integration procedure
=1 DIVON Integration procedure

`NCAL:` (D:=10000) Nr of calls per iteration for bases

`ACC1:` (D:=1) relative precision (in %) for grid optimisation

`ACC2:` (D:=0.5) relative precision (in %) for integration

6.2.1 Parameters for kinematics

`PLEPIN:` momentum p [GeV/c] of incoming electron (D=-30) (`/INPU/`)

`PIN:` momentum p [GeV/c] of incoming proton (D=820)(`/INPU/`)

`QMI:` (D: = 5.0) (`/DIFFR/`)Minimum Q^2 to be generated

`QMA:` (D: = 10^8) (`/DIFFR/`)Maximum Q^2 to be generated

`YMI:` (D: = 0.0)(`/DIFFR/`) Minimum y to be generated

`YMA:` (D: = 1.0) (`/DIFFR/`)Maximum y to be generated

`THEMA,THEMI` (D: `THEMA` = 180., `THEMI` = 0) maximum and minimum scattering angle θ of the electron (`/ELECT/`).

`NFLAV` (D: = 5) number of active flavors, can be set by user. (`/LUCO/`)

`NFLQCDC` (D: = 3) number of flavors allowed for QCD Compton processes, can be set by user (`/LUCO/`).

6.2.2 Parameters for hard subprocess selection

`IPRO:` (D: = 12) (`/RAPA/`) select hard subprocess to be generated. The selection of pomeron, pion or *standard* inelastic scattering is done via `IDIR`, `IDISDIF`, `NG`, `NPOM` described below.
=10: $\gamma g \to q\bar{q}$ using EPA
=11: $\gamma g \to c\bar{c}$ using EPA
=12: $eq \to e'q'$
=13: $eg \to e'q\bar{q}$ using full Matrix Element
=14: $eg \to e'Q\bar{Q}$ using full Matrix Element where Q is a heavy quark with flavor code set by `IHFLA` (D:`IHFLA=4`)
=15: $eq \to e'qg$ using full Matrix Element
=18: resolved photon processes. If `IHFLA > 3`, then only heavy quark production is siumulated with flavor given by `IHFLA`.
=20: $\gamma^* p \to q\bar{q}gp$ [56].
=21: $\gamma^* p \to q\bar{q}p$ [23, 24]. Exclusive diffractive dijet production, the same process as `IPRO=12` together with `NG=41` and `NPOM=41`, but technically calculated differently and more efficient.
=1200: use HERACLES [29, 30] (optional for simulation of QED radiation) for $eq \to e'q'$
=1400: use HERACLES [29, 30] (optional for simulation of QED radiation) for heavy quark production via boson gluon fusion: $eg \to e'Q\bar{Q}$

`Q2SUPP` (D=3.37) exponential low Q^2 suppression of the parton densities to be used with HERACLES: $1-\exp(-$`Q2SUPP`$\cdot Q^2$, can be changed by user (`/LOWQ2S/`).

`IDIR` (D: = 0) select type of events to be generated. (`/DISDIF/`)
= 1 *standard* inelastic scattering
= 0 diffractive and pion exchange processes

`IDISDIF` (D: = 0) choose mixing of *standard* inelastic scattering, diffractive and pion exchange processes according to cross section(`/DISDIF/`).
= 0 generates only the processes selected by `IDIR`. If `IDIR` = 0 then pomeron or pion exchange is selected via `NG` and `NPOM`.
= 1 mixing of *standard* inelastic and diffractive processes.
= 2 mixing of *standard* inelastic, diffractive and pion exchange processes.

`IFULL` (D: = 1) switch to select lowest order process (`IFULL` = 0) or quark parton model with $O(\alpha_s)$ matrix elements (`IFULL` = 1) (`/OALPINI/`).

`IQCDGRID` (D: = 1) switch to select generation of $O(\alpha_s)$ processes in a grid (`/OALPINI/`).

`INTER:` (D: =0) interaction type(`/INPU/`)
= 0 neutral current photon interaction
=2 charged current interaction

`SIN2W` (D:=0.23) for electroweak processes $\sin^2_W$ (`/EWEAK`).

`XMW2` (D:= $80 \cdot 80$ GeV^2) for electroweak processes m^2_W (`/EWEAK`).

`ISEMIH:` not used at present(`/INPU/`)

`PT2CUT(IPRO):` (D=5.0) minimum $\hat{p}^2_\perp$ for process `IPRO` (`/PTCUT/`). Must be used for generation of light quarks in processes `IPRO=10,13,15,18`.

6.2.3 Parameters for parton shower and fragmentation

`NFRAG:` (D: = 1) switch for fragmentation(`/INPU/`)
= 0 off
= 1 on
= 10 proton dissociation is switched on for all events

`IFPS:` (D: = 3) switch parton shower(`/INPU/`)
= 0 off
= 1 initial state
= 2 final state
= 3 initial and final state
= 10 gluon radiation according to ARIADNE.

`IORD:` (D: = 1) ordering for initial state P.S.
=0 no ordring
=1 Q^2 values at branches are strictly ordered, increasing towards the hard scattering strict ordered in Q^2
=2 Q^2 and opening angles of emitted (on shell or time like) partons are both strictly ordered, increasing towards the hard interaction as 1 but also strict ordered in angle

`IALP:` (D: = 1)
=1 α_s first order with scale Q^2
=2 α_s first order with scale $k_t^2 = (1-z) \cdot Q^2$

`ITIM:` (D: =1)
=0 no shower of time like partons
=1 time like partons may shower

`ISOG:` (D: =1) treatment of soft gluons
=0 soft gluons are entirely neglected
=1 soft gluons are resummed and included together with the hard radiation as an effective z shift

`KT1:` (D:=0.7) width of a gaussion for intrinsic k_t for photon

`KT2:` (D:=0.44) width of a gaussion for intrinsic k_t for proton

6.2.4 Parameters for resolved photon processes

process and color configuration for resolved photon processes (/COLCON/)

IRPA =1(0) (D:=1) process $gg \to q\bar{q}$ switched on(off)

IRPB =1(0) (D:=1) process $gg \to gg$ switched on(off)

IRPC =1(0) (D:=1) process $qg \to qg$ switched on(off)

IRPD =1(0) (D:=1) process $q\bar{q} \to gg$ switched on(off)

IRPE =1(0) (D:=1) process $q\bar{q} \to q\bar{q}$ switched on(off)

IRPF =1(0) (D:=1) process $qq \to qq$ switched on(off)

IRPG =1(0) (D:=0) process $qq \to qq$ (BFKL) switched on(off)

IHFLA flavor code IHFLA > 3 only heavy flavor production allowed (process IRPA and IRPE) (IHFLA = 4 for charm, IHFLA = 4 for bottom)

SCALQ2 (D:=1.) specifies the cut on $\frac{\mu^2}{Q^2}$ = SCALQ2 for resolved processes in DIS, can be changed by user (/RESGAM).

OMEG2: (D:=0.01) ω = OMEG2 suppression factor for virtual resolved photons in the Dress - Godbole model [40].

6.2.5 Parameters for structure functions α_s and scales

IRUNAEM: (D: = 0) select running of $\alpha_{em}(Q^2)$
=0: no running of $\alpha_{em}(Q^2)$
=1: running of $\alpha_{em}(Q^2)$

IRUNA: (D: = 1) switch for running α_s
=0: fixed $\alpha_s = 0.3$
=1: running $\alpha_s(\mu^2)$

IQ2: (D: = 5) select scale μ^2 for $\alpha_s(\mu^2)$
=1: $\mu^2 = 4 \cdot m_q^2$ (use only for heavy quarks!)
=2: $\mu^2 = \hat{s}$ (use only for heavy quarks!)
=3: $\mu^2 = 4 \cdot m^2 + p_\perp^2$
=4: $\mu^2 = Q^2$
=5: $\mu^2 = Q^2 + p_\perp^2$

SCALFA (D=1) (/SCALF/) factor which the scale μ^2 used in α_s and structure function evaluation is multiplied with. For example SCALFA=4 and IQ2=3 means: $\mu^2 = 4 \cdot m^2 + 4 \cdot p_\perp^2$, whereas for IQ2=5 the meaning is $\mu^2 = Q^2 + 4 \cdot p_\perp^2$.

MSTP(51): MSTP(51), MSTP(51) MSTP(56) is used to select structure function parameterizations (/PYPARS/). With MSTP(51) < 10 the parameterization of p structure function from PYSTFU are used:
= 0: Simple scaling Function
= 1: EHLQ set 1
= 2: EHLQ set 2
= 3: Duke-Owens set 1
= 4: Duke-Owens set 2
= 5: Morfin-Tung set 1 (S1)
= 6: Morfin-Tung set 2 (B1)

= 7: Morfin-Tung set 3 (B2)
= 8: Morfin-Tung set 4 (E1)
= 9: Gluck-Reya-Vogt LO set
= 10: Gluck-Reya-Vogt HO set
`MSTP(51)` > 10 parameterization from PDFLIB [6, 7] is used according to the following coding scheme:
1000000 $\times$ NPTYPE+1000 $\times$ NGROUP+NSET
example: 1003034 for NPTYPE 1 Ngroup 3 Nset 34 for MRS D- proton parton density.

`MSTP(52):` `MSTP(52)` < 10 parameterization of π structure function from `PYSTFU` (Owens set) is used
`MSTP(52)` > 10 parameterization from PDFLIB is used according to the following coding scheme:
1000000 $\times$ NPTYPE+1000 $\times$ NGROUP+NSET
example: 2005002 for NPTYPE 2 Ngroup 5 Nset 2 for GRV LO [25, 26] pion parton density.

`MSTP(56):` `MSTP(56)` < 10 inbuild parton densities are used:
= 1: GRS [38]
= 2: SaS [39]
`MSTP(56)` > 10 parameterization from PDFLIB is used according to the following coding scheme:
1000000 $\times$ NPTYPE+1000 $\times$ NGROUP+NSET
example: 3005002 for NPTYPE 3 Ngroup 5 Nset 2 for GRV [57] virtual photon parton density together with the Drees-Godbole Q^2 [40] suppression factor.

6.2.6 Parameters for diffraction

`NG:` (D: = -14) select pomeron structure function $xf(x)$ (`/DIFFR/`).
= 0: $xf_0(x) = 6x(1-x)$ for gluons. For quarks $xq(x) = \frac{1}{4}xf_0(x)$
= n: $xf_n(x) = (n+1)(1-x)^n$ for $1 \leq n \leq 5$ for gluons. For quarks $xq(x) = \frac{1}{4}xf_n(x)$
= 10: $xf(x) = (0.18 + 5.46x)(1-x)$ only gluons.
= 11: $xq(x) = \frac{1}{3}C\pi x(1-x)$ Donnachie Landshoff quark density in pomeron.
= 12: Kniehl, Kohrs, Kramer parton density [58, 59] for pomeron including direct coupling.
= 20: parton density for $\pi^{\pm}$. If `MSTP(52)` < 10 Owens set from PYSTFU is used. IF `MSTP(52)` > 10 parton density for pion used from PDFLIB [6, 7]
= 21: parton density for π^0. If `MSTP(52)` < 10 Owens set from PYSTFU is used. IF `MSTP(52)` > 10 parton density for pion used from PDFLIB
= 30: Nikolaev, Zakharov model [28].
= 40: Wüsthoff model [19].

= 41: Bartels, Lotter, Wüsthoff model [23, 24].
= 42: Diehl model [20, 21].
= 45: Buchmüller, Hebecker, McDermott model [27].
= -10: H1 fit 1 (quarks only) (NLO)[18]
= -11: H1 fit 2 (quarks and gluons) (NLO)[18]
= -12: H1 fit 3 (quarks and gluons peaked at $z \to 1$) (NLO)[18]
= -13: H1 fit 1 (quarks only)(LO) [18]
= -14: H1 fit 2 (quarks and gluons) (LO)[18]
= -15: H1 fit 3 (quarks and gluons peaked at $z \to 1$) (LO)[18]
< 0: user supplied structure function via subroutine `USDIFFR`. The parton density must be put in the array `XPQ(-6:6)` with the gluon at position 0, d, u, s, c, b, t quarks at positions $1, 2, 3, 4, 5, 6$ and the anti-quarks at $-1, -2, -3, -4, -5, -6$.

`NPOM:` (D: = -10) select pomeron distribution $f_{p/I\!P}$ (`/DIFFR/`)
= 0: pomeron distribution $f^S_{p/I\!P}$
= 1: pomeron distribution $f^{IS}_{p/I\!P}$
= 2: pomeron distribution $f^{DL}_{p/I\!P}$
= 20: $\pi^{\pm}$ t - distribution [60]
= 21: π^0 t - distribution [60]
= 30: Nikolaev, Zakharov model [28].
= 40: Wüsthoff model [19].
= 41: Bartels, Lotter, Wüsthoff model [23, 24].
= 42: Diehl model [20, 21].
= 45: Buchmüller, Hebecker, McDermott model [27].
= -10: H1 fit pomeron only [18]
= -11: H1 fit meson only [18]
= -12: H1 fit pomeron and meson [18]
< 0: user supplied pomeron distribution via subroutine `USDIFFR`.

Parameters for the diffractive gluon density in the semi-classical approach of Buchmüller, Hebecker, McDermott [27].

`C1:` (D: = 1) $C_1 =$ `C1` (`/BUCHMUE/`).

`Cg:` (D: = 1) $C_g =$ `Cg` (`/BUCHMUE/`).

`IREM:` (D: = 1) select momentum distribution of proton dissociation (`/PREMNANT/`).
= 1: $P(\beta') = 2(1-\beta')$
= 2: $P(\beta') = (a+1)(1-\beta')^a$
= 3: $P(\beta') = \frac{N}{\beta'\left(1-\frac{1}{\beta'}-\frac{c}{(1-\beta')}\right)^2}$

`IVM:` (D: = 0) select exclusive vector meson production in diffractive scattering (`/VMESON`).
= 0: no special selection done.
> 1 and < 443 :production of light vector mesons
= 443 :production of J/ψ mesons.
= 553 :production of Υ mesons.

`IALMKT:` (D: =0)(`/INPU/`) include primordial k_t for diffractive processes according to the Aligned Jet Model: $e^{-5.5k_t}$ for `IALMKT`=1 (`/INPU/`).

T2MAX: (D: = 5) maximum t [GeV$^2/c^2$] (/DIFFR/).
XF: (D: = 0.9) minimum XF $x_f = 1 - \frac{E'_p}{E_p}$ (/DIFFR/).
Parameters for pomeron flux (only for NPOM=0,1,2):
ALPHP: (D: = 0.25) $\alpha_{I\!P}$ [GeV^{-2}] (/DIFFR/).
RN2: (D: = 4.7) RN2= b_0 as defined above (/DIFFR/).
EPSP: (D: = 0.085) EPSP= ϵ (/DIFFR/).

6.2.7 Accessing information

AVGI	integrated cross section (/EFFIC/).
SD	standard deviation of integrated cross section (/EFFIC/).
SSS	total center of mass energy s (/PARTON/)
PBEAM	energy momentum vector of beam particles (/BEAM/)
KBEAM	flavor code of beam particles (/BEAM/)
Q2	in lepto-production: actual Q^2 of γ (/PARAE/).
YY	energy fraction lost by incident electron (/RAPGKI/)
XEL	energy fraction of parton on electron side (/RAPGKI/)
XPR	energy fraction of parton on proton side (/RAPGKI/)
YMAX,YMIN	actual upper and lower limits for y (/PARAT/).
Q2MAX,Q2MIN	actual upper and lower limits for Q^2 of γ (/PARAT/).
XMAX,XMIN	upper and lower limits for x (/PARAT/).
PT2H	$\hat{p}_\perp^2$ [GeV$^2/c^2$] of parton in hard subprocess cm (/RAPGKI/) system
SHH	invariant mass $\hat{s}$ [GeV^2] of hard subprocess (/RAPGKI/)
T2GKI	for diffractive processes T2GKI = t [GeV^2] (/RAPGKI/)
XFGKI	for diffractive processes XFGKI = $x_{I\!P}$ (/RAPGKI/)
	$O(\alpha_s)$ matrix element information (/MEINFO/)
AM(18)	vector of masses of final state particles of hard interaction.
SHAT	$\hat{s}$ of hard subprocess (/PARAT/)
ZQGKI	$z = \frac{p_i \cdot p_f}{p_i \cdot q}$ = ZQGKI (/MEINFO/)
XPGKI	$x_p = \frac{Q^2}{2p_i \cdot q}$ = XPGKI (/MEINFO/)
PHIGKI	ϕ = PHIGKI azimuthal angle (/MEINFO/)
NIA1,NIA2	position of partons in hard interaction in LUJETS event record (/HARD/)
NF1,NF2	first and last position final partons/particles of hard interaction in LUJETS (/HARD/)
NFT	total number of final particles; for $2 \to 2$ process NFT =2
Q2Q	hard scattering scale μ^2 used in α_s and structure functions (/PARAE/).
ALPHS	actual α_s (/PARAM/).
PI	π (/PARAM/).
ALPH	α_{em} (/PARAM/).
NIN	number of trials for event generation (/EFFIC/).
NOUT	number of successful generated events (/EFFIC/).
SCAL1,SCAL2	scale for structure function on beam 1 and 2 respectively (/STRU/).
XDP1,XPD2	value of parton density on beam 1 and 2 respectively (/STRU/).

6.3 List of COMMON blocks

```
COMMON/BEAM/PBEAM(2,5),KBEAM(2,5)
COMMON/BUCHMUE/C1,Cg
COMMON/COLCON/ICOLORA,IRESPRO,IRPA,IRPB,IRPC,IRPD,IRPE,IRPF,IRPG
COMMON/DIFFR/T2MAX,XF,ALPHP,RN2,EPSP,QMI,YMI,QMA,YMA,NG,NPOM
COMMON/DISDIF/IDIR,IDISDIF
COMMON/EFFIC/AVGI,SD,NIN,NOUT
COMMON/ELECT/THEMA,THEMI
COMMON/EWEAK/SIN2W,XMW2
COMMON/F2INT/F2DIS,F2DIF,F2PI COMMON/HARD/NIA1,NIR1,NIA2,NIR2,NF1,NF2,NFT
COMMON/INPU/PLEPIN,PPIN,NFRAG,ILEPTO,IFPS,IHF,IALMKT,INTER,ISEMIH
COMMON/LOWQ2S/Q2SUPP
COMMON/HFLAV/IHFLA
COMMON/LUCO/KE,KP,KEB,KPH,KGL,KPA,NFLAV,NFLQCDC
COMMON/MEINFO/ZQGKI,XPGKI,PHIGKI
COMMON/OALPINI/IFULL,IQCDGRID
COMMON/PARAE/Q2,Q2Q,PCM(4,18)
COMMON/PARAM/ALPHS,PI,ALPH,IWEI
COMMON/PARAT/AM(18),SHAT,YMAX,YMIN,Q2MAX,Q2MIN,XMAX,XMIN
COMMON/PARTON/SSS,CM(4),DBCMS(4)
COMMON/PREMNANT/IREM
COMMON/PTCUT/PT2CUT(100)
COMMON/PYPARS/MSTP(200),PARP(200)
PARAMETER (NY=40,NQ=20)
COMMON/QCDGRI/QY(NY),QQ(NQ),
& QPMDF(NY,NQ),QQBDF(NY,NQ),QQBHDF(NY,NQ),QCDCDF(NY,NQ),
& QPMPI(NY,NQ),QQBPI(NY,NQ),QQBHPI(NY,NQ),QCDCPI(NY,NQ),
& QPM(NY,NQ),QQB(NY,NQ),QQBH(NY,NQ),QCDC(NY,NQ)
PARAMETER (NBQ2=20,NBX=20)
COMMON/RAHER/IHERPYS,XPQDIF(-6:6,NBX,NBQ2),XPQPI(-6:6,NBX,NBQ2)
COMMON/RGRIDF2/XX(NBX),Q2X(NBQ2)
COMMON/F2VAL/F2_DIS(NBX,NBQ2),F2_DIF(NBX,NBQ2),F2_PI(NBX,NBQ2)
COMMON/RAPA/IPRO,IRUNA,IQ2,IRUNAEM,Q2START,W_Q2,OMEG2
COMMON/RAPGKI/YY,XEL,XPR,PT2H,SHH,T2GKI,XFGKI
COMMON/RESGAM/SCALQ2
COMMON/SCALF/SCALFA
COMMON/STRU/SCAL1,XPD1,SCAL2,XPD2
COMMON/VMESON/IVM
```

7 Example Program

```
      PROGRAM RGMAIN
```

```
      INTEGER IFULL,IQCDGRID
      COMMON /OALPINI/ IFULL,IQCDGRID
      INTEGER IDIR,IDISDIF
      COMMON/DISDIF/ IDIR,IDISDIF
      REAL PLEPIN,PPIN
      INTEGER KE,KP,KEB,KPH,KGL,KPA,NFRAG,ILEPTO,IFPS,IHF,IALMKT
      INTEGER INTER,ISEMIH
      INTEGER NIA1,NIR1,NIA2,NIR2,NF1,NF2,NFT,NFLAV,NFLQCDC
      COMMON/LUCO  /KE,KP,KEB,KPH,KGL,KPA,NFLAV,NFLQCDC
      COMMON/INPU  /PLEPIN,PPIN,NFRAG,ILEPTO,IFPS,IHF,IALMKT,INTER,
     +              ISEMIH
      COMMON/HARD/ NIA1,NIR1,NIA2,NIR2,NF1,NF2,NFT
      COMMON/HFLAV/ IHFLA
      REAL PARU,PARJ
      INTEGER MSTU,MSTJ
      COMMON/LUDAT1/MSTU(200),PARU(200),MSTJ(200),PARJ(200)
      INTEGER IWEI
      DOUBLE PRECISION ALPHS,PI,ALPH
      COMMON /PARAM/ ALPHS,PI,ALPH,IWEI
      DOUBLE PRECISION SIN2W,XMW2
      COMMON/ELWEAK/SIN2W,XMW2
      DOUBLE PRECISION PT2CUT,THEMA,THEMI,Q2START,W_Q2,OMEG2
      INTEGER IRUNA,IQ2,IRUNAEM
      INTEGER IPRO
      COMMON/RAPA /IPRO,IRUNA,IQ2,IRUNAEM,Q2START,W_Q2,OMEG2
      DOUBLE PRECISION SCALFA
      COMMON/SCALF/ SCALFA
      COMMON/PTCUT/ PT2CUT(20)
      COMMON/ELECT/ THEMA,THEMI
      REAL ULALPS,ULALEM
      EXTERNAL ULALPS,ULALEM
      PARAMETER (IPYPAR=60)
      REAL PARP
      INTEGER MSTP
      COMMON/PYPARS/MSTP(IPYPAR),PARP(IPYPAR)
      INTEGER NG,NPOM
      DOUBLE PRECISION T2MAX,XF,ALPHP,RN2,EPSP,QMI,YMI,QMA,YMA
      COMMON/DIFFR/T2MAX,XF,ALPHP,RN2,EPSP,QMI,YMI,QMA,YMA,NG,NPOM
      INTEGER IREM
      COMMON/PREMNANT/IREM
      COMMON/VMESON/IVM
      REAL PYPAR,PYVAR
      INTEGER IPY
      COMMON /PYPARA/ IPY(80),PYPAR(80),PYVAR(80)

C     initialize random number generator
```

```
      ISEED = 213123
      CALL H1RNIN(ISEED)
C---initialise RAPGAP parameters
      CALL GRAINI
C-- change standard parameters
C*********************************************************************
C     1ST INCOMING PARTICLE  (KE=11 ELECTRON)
C     1ST INCOMING PARTICLE  (KE=22 PHOTON)
      KE =  -11
c      KE =  22
C     LEPTON MOMENTIM (D=-30)
      PLEPIN = -27.5
C*********************************************************************
C     2ND INCOMING PARTICLE (KP = 2212 PROTON)
      KP = 2212
C     proton momentum (D=820)
      PPIN   = 820.
C*********************************************************************
C     PARTON SHOWER OFF/ON (D=10)
C     (off = 0, =1 initial state, =2 final state, =3 inital + final state
C       = 10 Ariadne)

      IFPS   = 1
C*********************************************************************
C     fragmentation on/off (D=1)
C     NFRAG=1         (D=1) FRAGMENTATION
C         =10 FRAGMENTATION+ p dissociation
      NFRAG  = 0
C     IREM=1   p dissociation treatment
C              (D=1): P(beta') = 2(1-beta')
C         =2        :          = (a+1)(1-beta')**a
      IREM = 1
C*********************************************************************
C     fixed/running alpha_s (D=1)
      IRUNA  = 1
C     alphas parameters
C     no of flavors wrt lambda_QCD
C     MSTU(112) = 5
C     lambda QCD
C     PARU(112) = 0.25
C     lambda QCD for MRSR2
C     PARU(112) = 0.239
C     min no of flavors for alphas
      MSTU(113) = 3
C     max no of flavors for alphas
```

```
      MSTU(114) = 5
C*********************************************************************
C      scale for alpha_s
C      1:  q2 = m**2
C      2:  q2 = shat
C      3:  q2 = m**2 + pt**2
C      4:  q2 = Q2
      IQ2    = 2
C*********************************************************************
C      scale factor q2 = SCALFA * q2
       SCALFA = 1.D0
C*********************************************************************
C     select process to be generated
c      WRITE(6,*) ' select process IPRO and IFULL,IDIR '
c      READ(5,*) IPRO,IFULL,IDIR
c      WRITE(6,*) ' IPRO = ',IPRO,' and event mixing IFULL = ',IFULL
c      write(6,*) ' IDIR = ',IDIR,' selected '
      IDIR = 1
      IPRO = 12
      IFULL = 0
C*********************************************************************
C  Processes gamma gluon fusion using EPA and gamma glu Matrix Element
C    10: gamma pomeron_gluon --> q qbar (light quarks:u,d,s)
C    11:  gamma pomeron_gluon --> Q Qbar (charm quarks)
C
C*********************************************************************
C  Process e q --> e' q'
C    12:  e q --> e' q'
C    1200:  e q --> e' q' using HERACLES
C*********************************************************************
C  Processes gamma gluon fusion using full e glu Matrix Element
C    13:  e pomeron_gluon --> e' q qbar (light quarks:u,d,s)
C    14:  e pomeron_gluon --> e' Q Qbar (charm quarks)
C    1400:  e pomeron_gluon --> e' Q Qbar (charm quarks) using HERACLES
C*********************************************************************
C  Process gamma* pomeron --> rho pomeron
C   100: e pomeron --> e' rho pomeron
C
C*********************************************************************
C    parameters for pomeron distribution
C     gluon density in pomeron (D=0)
C     (D=0) gluon density in pomeron
C     <0 user supplied via SUBROUTINE USDIFFR
C     20 = pion exchange
C     30 = Nikolaev Zakharov model
```

```
C     40 = hard pomeron M.Wuestoff
C     41 = hard pomeron  Bartels,Lotter,Wuesthoff
C     42 = 2 - glu pomeron(soft)  M.Diehl
      NG   =  0
C     if MSTP(52) < 10 use inbuilt structure functions of PYTHIA for pi
C if PDFLIB is used MSTP(51) gives
C     10^6*NPTYPE+1000*NGROUP+NSET    is used as coding scheme
C example 2001001 for NPTYPE 2 Ngroup 1 Nset 1
C      MSTP(52) = 2001001
C proton structure function
      MSTP(51) = 9
C
C
C     Q2SUPP=3.37  exponential suppression factor for small Q2
C               in parton densities for HERACLES
C               =5 for Q2 > 1
C               =10 for Q2 >0.5
      Q2SUPP = 3.37

C
C     NFLAV=5 no of flavors used in str.fct.
      NFLAV = 4
C     NFLQCDC=3 no of flavors allowed for QCD Compton processes
      NFLQCDC = 4
C
c photon structure function
c MSTP(56) = 1 GRS parameterization
c          = 2 SaSgam (Schuler-Sjostrand)
c          > 1000 PDFLIB with Drees Godbole virtual gamma suppression
      MSTP(56) = 1
C
C     SCALQ2=1. scale/Q2 for resolved gamma in DIS
      SCALQ2 = 1.0
C
C select pomeron distribution
C    (D=0) pomeron density
C  =0 Streng density ,
C  =1 Ingelman density,
C  =2 Donnachie Landshoff density,
C  =20 pion exchange
C  =30 Nikolaev Zakharov model
C  =40 hard pomeron M.Wuestoff
C  =41 hard pomeron  Bartels,Lotter,Wuesthoff
C  =42 2 - glu pomeron(soft)  M.Diehl
C  <0 user supplied via SUBROUTINE USDIFFR
```

```
      NPOM = 0
C epsilon for rising of x Section in Streng and DL pomeron distribution
      EPSP = 0.085
      RN2  = 4.0
      ALPHP = 0.25
C cut of x_f
      XF  = 0.9
c Maximum -t allowed in generation
      T2MAX = 1.
C
C     IALMKT=0   ( no primordial kt for partons in diffraction)
C           =1 ( primordial kt for partons for IPRO=12
C                 acc. aligned jet model)
      IALMKT=0
C
c select Vector meson production
c IVM = 1 light VM
C IVM = 443 J/psi
C IVM = 553 Upsilon
C IVM = 0 no special selection
      IVM = 0
C Minimum Q^2 of electron to be generated
      QMI = 0.5d0
C Minimum y of electron to be generated
      YMI=0.04d0
C pt^2_hat cut for light quark Matrix Elements
      PT2CUT(10)=1.
      PT2CUT(13)=1.
      PT2CUT(15)=1.
      PT2CUT(18)=4.
C Maximum theta angle of scattered electron
      THEMA = 180.0D0
C Minimum theta angle of scattered electron
      THEMI =   0.0D0
C switch off time like showers in pysspa
      IPY(14) = 1
C set lower energy for initial state PS
c      PYPAR(23)=1.
c select heavy flavor code for IPRO=14,1400
c      IHFLA=5
C*********************************************************************
C Initialize ARIADNE
      CALL ARINIT('RAPGAP')
C--- CALCULATE X SECTION
      CALL RAPGAP
```

```
C--- print x section
      CALL RAEND(1)
C--- event generation
      DO 10 I=1,5000
         CALL EVENT
C--- user analysis routine
         CALL ANALYS
C---
   10 CONTINUE
C---PRINT NO OF GENERATED EVENTS
      CALL RAEND(20)
      STOP
      END
```

8 Acknowledgment

I am grateful to T. Sjöstrand and G. Ingelman, the authors of PYTHIA and LEPTO for their permission to copy and use subroutines from their programs. All the credit concerning initial state parton showers and remnant treatment belongs to them.

I want to thank all those who continue-sly used and checked the program. Special thanks go to G. Briskin, A. Mehta and J. Philipps. Without their ideas, suggestions and comments and heavily use of the program, it would not be like it is now.

Without the great time and fun I still have with A. Daum it would have not been possible to search for free living pomerinos on the Canaries.

Index

References

[1] T. Sjöstrand, *Comp. Phys. Comm.* **39** (1986) 347.

[2] T. Sjöstrand, M. Bengtsson, *Comp. Phys. Comm.* **43** (1987) 367.

[3] T. Sjöstrand, *Comp. Phys. Comm.* **82** (1994) 74.

[4] B. Webber, Herwig 5.4, in *Proc. of the Workshop on Physics at HERA Vol. 3, 1354*, edited by W. Buchmüller, G. Ingelman (1991).

[5] S. Kawabata, *Comp. Phys. Comm.* **88** (1995) 309.

[6] H. Plothow-Besch, *Comp. Phys. Comm.* **75** (1993) 396.

[7] H. Plothow-Besch, *Int. J. Mod. Phys. A* **10** (1995) 2901.

[8] G. Ingelman, K. Prytz, *Z. Phys.* **C58** (1993) 285.

[9] H. Abramowicz, J. Bartels, L. Frankfurt, H. Jung, Diffractive Hard Scattering. Summary report of the working group, in *Proc. of the Workshop on Future Physics at HERA*, edited by A. De Roeck, G. Ingelman, R. Klanner (DESY, Hamburg, 1996), p. 635.

[10] G. Ingelman, P. Schlein, *Phys. Lett.* **B 152** (1985) 256.

[11] K. Streng, Hard QCD scatterings in diffractive reactions at HERA, in *Proc. of the Workshop Physics at HERA*, edited by R. Peccei (Hamburg, 1987).

[12] K. Streng, Hard QCD scatterings in diffractive reactions at HERA, 1988, CERN-TH 4949 (1988).

[13] E. Berger, J. Collins, D. Soper, G. Sterman, *Nucl. Phys.* **B 286** (1987) 704.

[14] P. Bruni, G. Ingelman, *Phys. Lett.* **B 311** (1993) 317.

[15] P. Bruni, G. Ingelman, Diffractive hard scattering at e p and p anti-p colliders, in *Proc. of the EPS International High Energy Physics Conference*, edited by J. Carr, M. Perrottet (Editions Frontieres, Marseille, France, 22-28 Jul, 1993), DESY 93-187.

[16] P. Bruni, G. Ingelman, A.Solano, Diffractively produced hadronic final states and the pomeron structure, in *Proc. of the Workshop on Physics at HERA, Vol. 1*, edited by W. Buchmüller, G. Ingelman (DESY, Hamburg, 1991), Vol. 311, p. 363.

[17] A. Donnachie, P. Landshoff, *Nucl. Phys.* **B 244** (1984) 322.

[18] H1 Collaboration; C. Adloff et al., *Z. Phys.* **C 76** (1997) 613.

[19] M. Wusthoff, Photon diffractive dissociation in deep inelastic scattering, 1995, PhD thesis, DESY-95-166.

[20] M. Diehl, Diffraction in electron - proton collisions, 1996, PhD thesis.

[21] M. Diehl, *Z. Phys.* **C 76** (1997) 499, hep-ph/9610430.

[22] J. Bartels et al., Quark - Antiquark Jets in DIS Diffractive Dissociation, in *Proc. of the Workshop on Future Physics at HERA*, edited by A. De Roeck, G. Ingelman, R. Klanner (DESY, Hamburg, 1996), hep-ph/9609239.

[23] J. Bartels, H. Lotter, M. Wüsthoff, *Phys. Lett.* **B 379** (1996) 239, hep-ph/9602363.

[24] J. Bartels, C. Ewerz, H. Lotter, M. Wusthoff, *Phys. Lett.* **B 386** (1996) 389, hep-ph/9605356.

[25] M. Glück, E. Reya, A. Vogt, *Z. Phys.* **C 53** (1992) 127.

[26] M. Glück, E. Reya, A. Vogt, *Phys. Lett.* **B 306** (1993) 391.

[27] W. Buchmuller, M. McDermott, A. Hebecker, *Nucl. Phys.* **B 487** (1997) 283, hep-ph/9607290.

[28] N. Nikolaev, B. Zakharov, *Z. Phys.* **C 53** (1992) 331.

[29] A. Kwiatkowski, H. Spiesberger, H.-J. Möhring, HERACLES 4.1 - An event generator for *ep* interactions at HERA including radiative processes, in *Proc. of the Workshop on Physics at HERA, Vol. 3*, edited by W. Buchmüller, G. Ingelman (1991), p. 1294.

[30] A. Kwiatkowski, H. Spiesberger, H.-J. Möhring, *HERACLES - An event generator for ep interactions at HERA including radiative processes. version 4.6*, 1996, `http://www.desy.de/~hspiesb/heracles.html`.

[31] V. Gribov, L. Lipatov, *Sov. J. Nucl. Phys.* **15** (1972) 438 and 675.

[32] L. Lipatov, *Sov. J. Nucl. Phys.* **20** (1975) 94.

[33] G. Altarelli, G. Parisi, *Nucl. Phys.* **B 126** (1977) 298.

[34] Y. Dokshitser, *Sov. Phys. JETP* **46** (1977) 641.

[35] H. Plothow-Besch, PDFLIB Version 7.09, User's Manual. W5051 1997.07.02 CERN-PPE, 1997.

[36] J. Chyla, J. Cvach, Virtual Photon Structure from jet production at HERA, in *Proc. of the Workshop on Future Physics at HERA*, edited by A. De Roeck, G. Ingelman, R. Klanner (Hamburg, 1996).

[37] H. Jung, *Comp. Phys. Comm.* **86** (1995) 147.

[38] M. Glück, E. Reya, M. Stratman, *Phys. Rev.* **D 54** (1996) 5515.

[39] G. Schuler, T. Sjöstrand, *Phys. Lett.* **B 376** (1996) 193.

[40] M. Drees, R. Godbole, *Phys. Rev.* **D 50** (1994) 3124.

[41] E. Mirkes, D. Zeppenfeld, *Phys. Lett.* **B 380** (1996) 105.

[42] S. Catani, M. Seymour, NLO QCD calculations in DIS at HERA based on the dipole formalism, in *Proc. of the Workshop on Future Physics at HERA*, edited by A. De Roeck, G. Ingelman, R. Klanner (Hamburg, 1996).

[43] M. Klasen, G. Kramer, B. Potter, *Eur. Phys. J.* **C C1** (1998) 261, hep-ph/9703302.

[44] G. Ingelman, LEPTO 6.1 The Lund Monte Carlo for deep inelastic lepton-nucleon scattering, in *Proc. of the Workshop Physics at HERA (1991) Vol. 3, 1366*, edited by W. Buchmüller, G. Ingelman (DESY, Hamburg, 1991).

[45] G. Briskin, phD Thesis , changing LUKFDI for vm production.

[46] H1 Collaboration; S. Aid et al., *Nucl. Phys.* **B 468** (1996) 3.

[47] J. Breitweg et al., *Z. Phys.* **C 75** (1997) 215, hep-ex/9704013.

[48] H. Jung, Modelling Diffractive Processes, in *Proc. of the Workshop on Diffractive Interactions*, edited by A. Levy (Eilat, Israel, Feb. 18 - 23, 1995).

[49] L. Lönnblad, *Comp. Phys. Comm.* **71** (1992) 15.

[50] G. Ingelman, A. Edin, J. Rathsman, *Comp. Phys. Comm.* **101** (1997) 108.

[51] M. H. Bengtsson, *Comp. Phys. Comm.* **31** (1984) 323.

[52] T. Sjöstrand, *Phys. Lett.* **B 157** (1985) 321.

[53] M. Bengtsson, T. Sjöstrand, M. van Zijl, *Z. Phys.* **C 32** (1986) 67.

[54] H1 Collaboration; I. Abt et al., *Z. Phys.* **C 63** (1994) 377, DESY 94-033.

[55] M. Bengtsson, T. Sjöstrand, *Z. Phys.* **C 37** (1988) 465.

[56] J. Bartels, qqg jets in diffraction, in *Proc. of the LISHEP workshop on diffractive physics*, edited by A. Santoro (Rio de Janeiro, Brazil, Feb 16 - 20, 1998).

[57] M. Glück, E. Reya, A. Vogt, *Z. Phys.* **C 53** (1992) 127.

[58] H. Kohrs, Direct and resolved pomeron, in *Proc. of the Workshop on Deep Inelastic Scattering and QCD*, edited by J. Laporte, Y. Sirois (1995).

[59] B. Kniehl, H. Kohrs, G. Kramer, *Z. Phys.* **C 65** (1995) 657.

[60] H. Holtmann et al., *Phys. Lett.* **B 338** (1994) 363.